Designing a Reproducible Endothelialized Channel in a 3D Hydrogel to Model Cerebral Cavernomas in Vitro

Authors:
Zoe Leak
Autumn Birch

Department of Biomedical Engineering
University of Virginia ` Charlottesville, Virginia
Spring 2025

Word Count: 3261
Number of Figures: 4
Number of Tables: 1
Number of Equations: 0
Number of Supplements: 7
Number of References: 12

Faculty Advisor
Brian Helmke, Biomedical Engineering
Faculty Advisor Signature

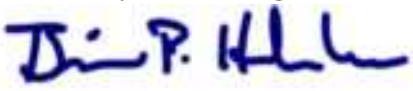

Designing a Reproducible Endothelialized Channel in a 3D Hydrogel to Model Cerebral Cavernomas in Vitro

Zoe A. Leak[a], Autumn L. Birch[b]

[a] UVA Department of Biomedical Engineering, Undergraduate
[b] UVA Department of Biomedical Engineering, Undergraduate
* The authors contributed equally to this work

Abstract

Cerebral Cavernous Malformations (CCMs) are vascular anomalies that disrupt endothelial barrier integrity, resulting in heightened vascular permeability and severe neurological complications. Existing in vivo models struggle with reproducibility and translational accuracy. To address these gaps, we developed an in vitro model using a Norbornene-Modified Hyaluronic Acid (NorHA) hydrogel with a perfusable channel mimicking cerebral capillaries. Rheological characterization was conducted to tune the hydrogel's mechanical properties to match brain tissue. We designed a reproducible fabrication process using 3D-printed molds and PDMS scaffolding. Bovine Aortic Endothelial Cells (BAECs) were cultured on hydrogel slabs and within channels to assess adhesion and potential for monolayer formation. Rheological analysis demonstrated that a 2% NorHA formulation closely matched the brain tissue's target storage (600–1100 Pa) and loss moduli (350–600 Pa). Slab adhesion studies indicated promising compatibility for endothelial monolayer formation, with imaging throughout incubation revealing that the 3% NorHA hydrogel retained more cellular adhesion over the 2% NorHA hydrogel slab. Preliminary FITC-dextran diffusion tests suggested the hydrogel's capacity to differentiate between cell-lined and unlined permeability profiles. This study presents a scalable and repeatable in vitro platform for studying endothelial behavior under physiologically relevant conditions. Our system holds future potential for further parameter optimization and modeling genetic modifications, such as KRIT-1 knockdown, to explore CCM lesion progression.

Keywords: NorHA, Hydrogel Fabrication, Rheology, Cerebral Cavernous Carcinoma

Introduction

Cerebral cavernous malformations (CCMs) are the second most prevalent finding in magnetic resonance images (MRIs) of the brain (Caton & Shenoy, 2024). CCMs are irregularly mulberry-shaped clusters of enlarged blood vessels in the central nervous system. CCMs can cause inflammation, seizures, headache, hemorrhage, and focal neurological deficits, including stroke (National Institute of Neurological Disorders and Stroke, 2024).

This cardiovascular disease (CVD) affects the function of endothelial cells by disrupting their ability to form cell-to-cell junctions and increasing the endothelial layer's permeability (Awad & Polster, 2019). Endothelial cells (ECs), make-up the monolayer lining between the bloodstream and its surrounding tissue, controlling nutrient exchange vital for proper life functioning. However, literature so far has only identified a link between loss-of-function in proteins encoded by three genes and the initial development of CCM (Sahoo et al., 1999). These three genes are the Krev Interaction Trapped-1 (KRIT-1), Malcavernin, and PDCD10. Fischer et al (2013) hypothesized that CCM functions using Knudson's two-hit mechanism: the first "hit" causing CCM formation is a loss-of-function mutation of one of the three implicated genes, and the second "hit" is unknown.

From blood flow along the wall of the vessel, atherosclerotic lesions have been shown to prevail (Caro et al., 1969). This may also be true for CCM lesions. CCM has previously been studied in mouse models (in vivo). However, due to the variability between models, it is difficult to study endothelial cellular mechanisms and their response to shear stress in vivo (Maderna et al., 2022). To address the limitations of current in vivo models and explore the cellular mechanisms underlying CCM lesion formation, we hypothesized that an in vitro hydrogel-based platform could replicate the cerebral microenvironment with sufficient mechanical fidelity and biological compatibility to support endothelial function and permeability assays.This technical project aims to aid in identifying the role of shear stress in CCM formation through a platform of a reproducible model outside of a living organism (in vitro). While conventional lab models confine cells to flat 2D surfaces, true anatomy tells a different story - blood vessels are intricate 3D highways where flow dynamics shape cellular behavior. Through the use of 3D biomaterials, such as biocompatible hydrogels, in vitro models that more accurately depict the true environment of tissue microvasculature functions can be constructed.

Hydrogels have emerged as a powerful platform for engineering tissues and organs, owing to their unique polymer networks and high water content (Lee et al., 2023). These versatile materials can be engineered to replicate the extracellular matrix, which regulates cell function, by incorporating cell-adhesion biochemical ligands. Ligands, like arginine-glycine-aspartate (RGD), are essentially hand holds for cells to facilitate cellular attachment and integration (Bellis, 2011). Our approach utilizes a Norbornene-Modified Hyaluronic Acid (NorHA) Ultra Violet (UV) crosslinked hydrogel. Through careful adjustment of norbornene polymer concentration, we can achieve mechanical stiffness properties matching those of brain tissue, specifically targeting between 600 -1100 Pascals (Pa) for storage modulus and 350 - 600 Pa for loss modulus (Fallenstein et al., 1969). The fabrication process involves combining NorHA with RGD peptides, casting the solution in custom 3D-printed molds, penetrating a 22-gauge needle, and initiating crosslinking via UV exposure to create the final structure. The needle mimics the average diameter of a cerebral blood vessel (<1mm). The UV exposure curing is a form of photocrosslinking that provides an inert and uncontaminated structure for seeded cells to proliferate and form a monolayer in the hydrogel.

Introducing a fluorescein isothiocyanate (FITC)-conjugated dextran dye in the solution to perform a permeability assay will provide the baseline measurement of the hydrogel's perfusability. Bovine aortic endothelial cells (BAECs) will be cultured on culture-treated plastic in 2D until they reach an 80% confluency, to ensure a sufficient cell count to form a confluent monolayer. Although BAECs are harvested from cow heart cells, they are used because they are easily accessible, maintainable, and cost efficient.

Guided by prior capstone work and literature, our design strategy focused on three core objectives: (1) engineer a NorHA hydrogel with brain-like viscoelastic properties, (2) fabricate a perfusable microchannel capable of supporting molecular diffusion, and (3) evaluate initial endothelial cell adhesion within the hydrogel system. Further development and iterations of this in vitro model hold promise to revolutionize our understanding and treatment of CVD as a whole. Beyond providing a platform for testing new drugs and personalized genetic therapies, this reproducible system offers a window into the fundamental cellular behaviors that underlie CCM's pathology.

Results

Rheology

In order to determine the hydrogel composition that resulted in the mechanical properties that most accurately mimicked brain tissue, rheology testing was performed on 2% and 3% NorHA concentration hydrogels. Comprehensive rheology testing revealed that the 2% NorHA concentration more closely matched our target mechanical properties of brain tissue. Rheology testing measures the fluid-like and elastic properties of materials. The loss modulus represents the permanent structural change within the material as a result of applied stress, and the storage modulus is a measure of a material's stiffness, or its ability to store energy elastically. Our rheology testing involved both an amplitude sweep and frequency, however, we ultimately used the data obtained from the amplitude sweep, which plots these moduli across oscillation strain. The amplitude sweep measurements for the 2% concentration showed an average storage modulus of 1627.79 Pa and an average loss modulus of 169.75 Pa. The measurements for the 3% concentration showed an average storage modulus of 2144.80 Pa and a loss modulus of 198.01 Pa. The 2% most closely resembles the values that fall within our target storage modulus range of 600 - 1100 Pa and loss modulus range of 350 - 600 Pa, determined from established literature values (Fallenstein et al., 1969). Our results concur with expectations as the 3% NorHA hydrogel presented with a higher storage modulus, confirming its increased stiffness (Table 1b). Additionally, the 2% hydrogel presented with the higher loss modulus, confirming its dampening and softer properties as it has a lower concentration of NorHA (Table 1a).

	2% NorHA Concentration	
	Storage Modulus (Pa)	Loss Modulus (Pa)
Trial 1	1308.05	183.51
Trial 2	1276.61	103.46
Trial 3	2298.72	222.28
Average	**1627.79**	**169.75**

Table 1a. Rheological results for 2% NorHA hydrogels

	3% NorHA Concentration	
Trial 1	1498.11	117.17
Trial 2	2695.59	176.13
Trial 3	2240.69	300.72
Average	**2144.80**	**198.01**

Table 1b. Rheological results for 3% NorHA hydrogels

Endothelial Cell Seeding in Channels and Flat Hydrogels

The first cell seeding experiment occurred in a 2% NorHA hydrogel channel in the PDMS mold with wells (Figure S3). Initial seeding images indicated an approximately 30% cell density in the channel with a significantly higher confluency in the wells. The seeded hydrogel was imaged at initial injection and 2 hours after incubation (Figure 1a and 1b).

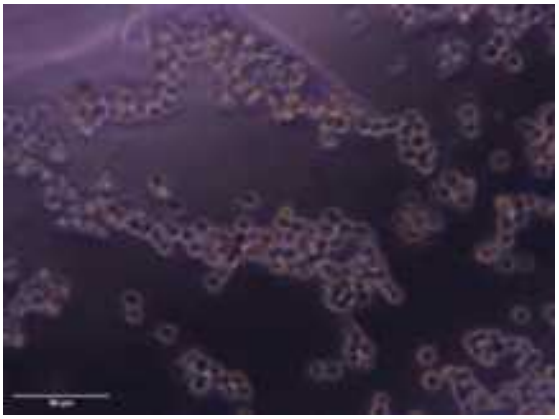

Figure 1a. Microscopic image of cells after initial injection in the 2% NorHA hydrogel channel

Figure 1b. Microscopic image of cells after a 2-hour incubation period in the 2% NorHA hydrogel channel

We initially intended to capture images every 2 hours; however, after reviewing the results after the 2-hour incubation period, we concluded that there was a significant reduction in cells and no

adherence or monolayer formation present, therefore, the experiment needed to be reevaluated.

In order to determine the true biocompatibility of the hydrogel with BAECs, we elected to conduct a cell seeding experiment on a slab of hydrogel rather than within a hydrogel channel. A cell media solution was placed on sterile 2% and 3% hydrogels, incubated and imaged. Initial imaging showed good initial confluency and increased adherence over time (Figure 2). Although adherence was visually confirmed, results regarding monolayer formation were inconclusive. The 0-hour images highlight cells possessing a circular shape with more dispersion. With each increasing time point until the 20-hour mark we observed cells increasingly packed together; a higher density can be assumed as less light is reflecting through the microscope and ultimately into the image which is why the cells appear darker.

	0 hour	**0.5 hour**	**5 hour**	**20 hour**
2% NorHA Hydrogel				
3% NorHA Hydrogel				

Figure 2. Microscopic images of cells on a 2% and 3% NorHA hydrogel sheet after various incubation periods

FITC-dextran Diffusion Results

To characterize the baseline permeability of our hydrogel constructs, we introduced 40 kDa FITC-dextran into unseeded hydrogel channels and monitored fluorescence diffusion over a 30-minute period using fluorescence microscopy. The channels were fabricated from both 2% and 3% NorHA formulations and crosslinked around a 22G needle to produce straight, cylindrical lumens.

Fluorescence images were acquired over time post-injection (Figure 3). The green lines indicate the locations the measurements were obtained from. The diffusion of FITC-dextran was visualized across the width of the hydrogel and analyzed using ImageJ to quantify fluorescence intensity as a function of distance from the center of the channel. The most representative and artifact-free trial was observed in the 3% NorHA hydrogel, which maintained lumen integrity and minimized structural tears or deformation that could interfere with diffusion measurements.

An intensity vs. distance profile was generated for this 3% NorHA trial by averaging selected regions of interest along the channel axis (Figure 4). The fluorescence gradient demonstrated clear outward diffusion over time, with increasing distance correlating to decreasing FITC intensity.

However, due to multiple factors including background noise, nonuniform light scattering, and the absence of a fluorescence calibration curve, the absolute permeability coefficient could not be calculated. Nevertheless, the profiles provided qualitative evidence that the hydrogel matrix restricted but permitted molecular diffusion, and the degree of diffusion observed is consistent with previous reports on hydrogel porosity.

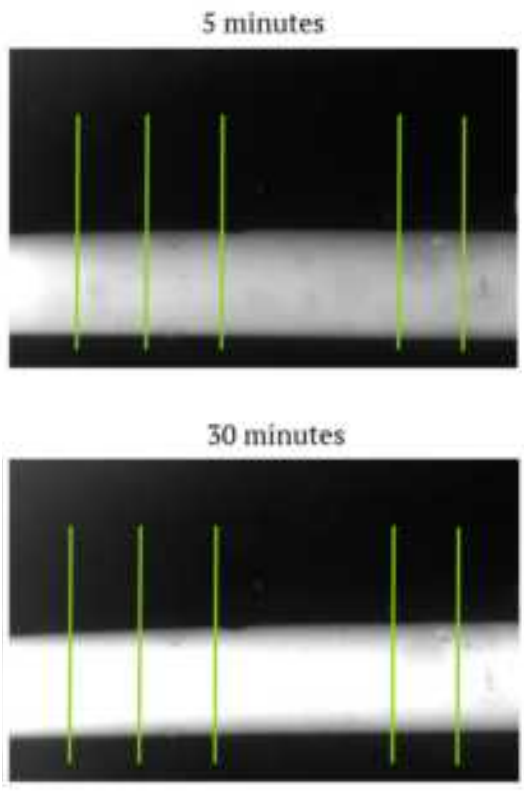

Figure 3: The hydrogel channel after FITC-dextran injection, imaged at different time points at a 50-ms exposure time.

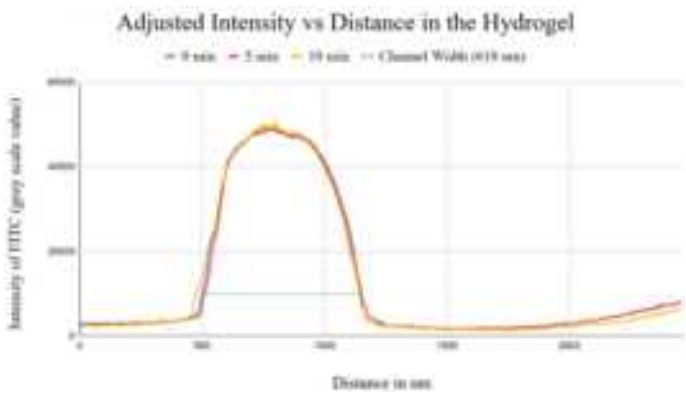

Figure 4: Intensity vs Distance across the hydrogel graph depicts a relatively uniform intensity across the gel for the different time points. The zero x and y points represent the bottom of the green line, from which the intensity data was drawn from by averaging the values of the 5 lines

Discussion

Our hydrogel formulation decisions were guided by both a review of existing literature and the methodology established by a prior capstone project conducted by Lauren Porter. Specifically, the previous student investigating CCM used 2% NorHA for its biocompatibility and storage modulus proximity to brain tissue mechanical properties. Literature also consistently identifies brain tissue to have storage moduli between 600–1100 Pa and loss moduli between 350–600 Pa (Fallenstein et al., 1969; Lee & Mooney, 2001). These values formed the cornerstone of our material design criteria.

Beyond material formulation, significant design considerations went into the geometry and function of our in vitro system. We developed two CAD designs for our PDMS molds: one with adjacent wells on either side of the hydrogel channel and one without wells. The version without wells was designed for initial hydrogel polymerization and rheological testing, maximizing simplicity and minimizing fluid loss. In contrast, the mold with wells was developed specifically for cell culture applications, enabling the accumulation of cell media adjacent to the hydrogel and maintaining hydration and nutrient diffusion over extended periods. This design choice reflects a tradeoff between ease of fabrication and functional utility. The inclusion of wells made the device more compatible with long-term cell viability and provided a more realistic vascular niche for BAECs. The ability to isolate the cell media from environmental evaporation also improved sterility and reduced variability.

Importantly, the addition of wells served a biological and experimental purpose beyond just fluid containment. These wells were designed to act as depositories for excess BAECs and cell culture media. Our cell seeding strategy intentionally involved injecting a volume of suspended cells that exceeded the amount needed to fully cover the interior surface area of the hydrogel channel. This was based on the assumption that not all injected cells would adhere to the hydrogel walls; some would either die or remain in suspension. The adjacent wells allowed for those non-adherent cells to settle without increasing crowding within the channel, thereby minimizing the risk of cellular shear-off or detachment from the luminal wall.

Additionally, the presence of extra cell media in the wells supported nutrient diffusion and broader spatial access to metabolites needed for proliferation and maintenance of viable endothelial monolayers. This design consideration helped simulate physiological conditions in which endothelial cells exist in a perfused, nutrient-rich environment and offered a more stable experimental setup for prolonged culture. The wells thus enhanced both the biological realism and robustness of the in vitro system.

This work provides the foundational framework for developing a physiologically relevant in vitro model to investigate the role of endothelial dysfunction in CCM. By tuning the stiffness of NorHA hydrogels and designing reproducible fabrication and testing methods, we successfully achieved partial cell adhesion and hydrogel perfusability. However, the findings also illuminated several critical nuances and limitations that shape the interpretation of our results and guide future iterations.

Looking at the apparent inconsistency between rheological optimization and biological response. Although 2% NorHA demonstrated storage and loss moduli more consistent with brain tissue (1308.05 Pa and 183.51 Pa, respectively), initial qualitative imaging showed that BAECs appeared to adhere more favorably to the stiffer 3% NorHA slabs. This paradox highlights the complexity of biomaterial-cell interactions. One hypothesis is that while the 2% gel more closely mimics native brain stiffness, it may lack sufficient mechanical integrity to support strong focal adhesion formation in BAECs, which are derived from large vessel endothelium and may inherently prefer stiffer substrates(Andresen Equiluz et al., 2017). Additionally, the increased matrix density in 3% NorHA could present more adhesive contact points or slower degradation, promoting improved cell retention even at the cost of reduced physiological mimicry.

This finding suggests that there is no universally ideal hydrogel formulation, rather, the optimal stiffness may depend on the specific endothelial phenotype and experimental goals (Yi et al., 2022). Future groups should explore a broader range of NorHA concentrations, including 4%, 5%, or even 6%, to map out whether there is a threshold stiffness beyond which endothelial cell proliferation and confluency are maximized. Conversely, testing lower concentrations, such as 1.5%, might reveal a failure point for structural integrity in soft hydrogels.

Another important conclusion involves the challenges associated with cell adhesion in 3D channel environments. Despite our successful slab trials, full endothelialization within the perfusable channels was not achieved. This may result from multiple technical factors: suboptimal surface chemistry, incomplete sterilization, or the limited residence time of suspended cells in contact with the channel wall. Moreover, BAECs seeded under static conditions may not receive enough directional cues to organize into a confluent monolayer. In future iterations, implementing a rotation protocol, applying low shear preconditioning flow, or supplementing with extracellular matrix proteins like fibronectin could enhance uniformity.

While the results in the preliminary FITC-dextran permeability assays were not quantified, they support the feasibility of using this platform to assess barrier function in response to endothelial integrity. Future experiments should include a standardized time-lapse imaging protocol, image segmentation using ImageJ, and fluorescence intensity normalization to calculate permeability coefficients using Fick's Law.. However, it is important to clarify that our FITC-dextran assays were conducted exclusively on acellular hydrogel channels, and not in conjunction with any cell-seeded constructs. The objective of these trials was to evaluate the baseline permeability characteristics of the NorHA hydrogel. We did not collect fluorescence calibration curves, which limited our ability to translate fluorescence intensity into absolute concentration values, thereby precluding true permeability coefficient calculations. Instead, we relied on visual assessments of diffusion gradients to infer permeability differences.

The most promising FITC-dextran trial was conducted using a 3% NorHA hydrogel, where the cylindrical channel appeared straight, free of tears, and minimally affected by imaging artifacts. Despite these ideal physical conditions, data analysis revealed substantial signal noise. Even after carefully selecting regions of interest that avoided visible imaging distortions and heterogeneity within the channel, the resulting fluorescence intensity profiles were too variable to reliably characterize the hydrogel's permeability.

Future groups should incorporate a more thorough quantitative framework for permeability measurement, beginning with the construction of calibration curves to correlate intensity to known FITC-dextran concentrations. They should also perform multiple replicates and apply time-lapse imaging protocols to derive accurate diffusion coefficients. Improvements in imaging consistency, such as using lower-autofluorescence materials and background correction methods, will be crucial for obtaining interpretable and reproducible results. Additionally, cross-validating permeability values through orthogonal techniques such as transwell assays or fluorescence recovery after photobleaching (FRAP) may strengthen conclusions.

In reviewing the fluorescence images from our FITC-dextran assays, we observed several imaging artifacts that may have introduced noise into our preliminary interpretations. These artifacts included uneven background fluorescence, minor channel leakage, and irregular light scattering at the channel edges, likely caused by hydrogel surface roughness and PDMS autofluorescence. Such artifacts compromise the clarity of intensity gradients and can misrepresent actual diffusion profiles.

To address this in future studies, it will be essential to implement standardized imaging parameters, including flat-field correction, and to use low-autofluorescence materials for scaffolds. Additionally, enclosing the imaging environment to minimize ambient light interference and incorporating calibration beads could assist in correcting for uneven illumination or focal drift. Improved image processing pipelines, like using automated segmentation and background subtraction in ImageJ, can further enhance the fidelity of fluorescence quantification. Including multiple replicates and normalizing signal across trials will be critical for robust permeability coefficient extraction.

Long-term, this platform holds promise for simulating disease-specific conditions. Once channel endothelialization is optimized, one may introduce KRIT-1 knockdown via siRNA transfection in BAECs. Comparing permeability in wild-type versus CCM-phenotyped channels under constant flow (10 dyne/cm²) allows for directly testing the impact of genetic perturbation on endothelial barrier function. With sufficient validation, this system may serve as a platform for preclinical drug screening and pathophysiological analysis in CCM and related cerebrovascular disorders.

Materials and Methods

Hydrogel Fabrication

This project utilized Norbornene-modified hyaluronic acid (NorHA) hydrogels due to its biocompatibility with cells and easy hydrogel formation. A 36% DMTMM Modified NorHA is initially dissolved in DI water and combined with 25 mg/mL Dithiothreitol (DTT) and 10 mM PBS diluted Lithium phenyl(2,4,6-trimethylbenzoyl)phosphinate (LAP). DTT is a reducing agent that breaks the disulfide bond and halts crosslinking based on the concentration. LAP is a photoinitiator that initiates the crosslinking by absorbing photons introduced by the blue UV light. These ingredients are vortexed and crosslinked under a UV lamp for 5 minutes at 15 milliwatts to produce our hydrogel.

Hydrogel Channel Formation

Channels are created using a 22-gauge needle inserted into the PDMS mold. The needle is placed through the holes of the mold, the hydrogel solution is placed and cured around it (Figure S7). The needle is then gently removed from the hydrogel, leaving a cylindrical channel with a diameter of approximately 0.718mm.

CAD Design and PDMS Protocol

Molds are produced using CAD software and printed using a resin printer. The diameter of the resin printed channel is slightly increased to allow for easy entry and removal of the 22-gauge needle (Figure S4). An additional iteration was generated to include wells for cell media when conducting cell experiments (Figure S5). Polydimethylsiloxane (PDMS) is then procured and poured into the resin molds, around a 21-gauge needle, to sit and cure in a 37° oven. Once solidified, the PDMS mold is pulled from the resin mold and plasma bonded to a glass slide for experimental use.

Endothelial seeding and sterilization process

Hydrogel-cell experiments involve a hydrogel sterilization process and cell introduction. Our PDMS device is sterilized in IPA and washed with PBS. Under a biosafety hood, a sterile NorHA hydrogel is formulated with the addition of RGD peptides, which promote cell adhesion, migration, and survival. The sterile hydrogel mixture is placed into the sterile device and cured under the UV lamp within a sealed container to maintain sterility. Bovine Aortic Endothelial Cells (BAECs) were selected for our cell seeding experiments due to their hardiness and biocompatibility with hydrogel properties. BAECs were cultured and passaged throughout the duration of our project and used once a T-25 flask approached 70-90% confluency. Cells were lifted and counted to ensure a cell number of ~3 million cells, as that accounted for the total surface area of the channel and the surrounding wells. The cells were diluted in 1 mL of media, the solution was horizontally injected into the hydrogel, and introduced into the wells using a syringe and needle. The product is then incubated and imaged over time to track cell adhesion and proliferation.

FITC-dextran System

To assess baseline hydrogel permeability, acellular channels were perfused with 40 kDa FITC-dextran (0.5 mg/mL) diluted in PBS. The FITC-dextran was introduced through inlet tubing using a syringe to ensure minimal injection variability. The injection was performed slowly to fill the cylindrical channel without disrupting the hydrogel matrix. Channels were then sealed and imaged using fluorescence microscopy.

Fluorescence images were captured at different time intervals using a microscope equipped with a 495 nm excitation filter. Imaging was conducted under consistent exposure and gain settings to ensure comparative analysis. ImageJ was used to analyze the resulting fluorescence distribution by plotting intensity values as a function of distance from the channel center. Regions of interest were selected to avoid artifacts and edge effects.

Despite efforts to standardize analysis, the absence of a fluorescence calibration curve prevented absolute quantification of FITC concentration or the calculation of true permeability coefficients. The diffusion patterns were interpreted qualitatively, serving as a visual metric of molecular transport through the hydrogel matrix. The most successful trial was obtained in a 3% NorHA hydrogel, where the channel was structurally intact, exhibited minimal tearing, and yielded the most uniform diffusion gradient for visualization. Future

experiments should implement quantitative calibration with serially diluted FITC-dextran standards, multiple replicate trials, and automated background subtraction. These improvements would allow for more precise, reproducible permeability measurements using Fick's Law.

While our platform remains a prototype, its conceptual framework aligns with innovations being pursued in other leading tissue engineering laboratories. For instance, Dr. Wilbur Lam's lab at Georgia Tech has made notable progress using microfluidic systems to mimic vascular barriers and study disease states. Their endothelialized hydrogel models enable accurate recapitulation of physiological permeability and cell interactions in engineered blood-brain barrier constructs (Qiu et al., 2018). Similarly, Dr. Steven Caliari's group at the University of Virginia has employed NorHA-based hydrogel patterning techniques to achieve spatially defined cell environments that guide endothelial organization and matrix remodeling—demonstrating control over mechanical and biochemical microenvironments through light-mediated fabrication strategies (Skelton et al., 2024). These efforts illustrate the critical role of hydrogel design and spatial patterning in achieving biologically relevant behavior in vitro.

By comparison, our model represents an early-stage but modular approach to constructing perfusable hydrogel systems with design features tailored for permeability analysis and disease modeling. While we have not yet reached the level of precision or cellular integration demonstrated by Lam or Caliari's teams, the core methodologies—NorHA chemistry, controlled photopolymerization, and vascular mimicry—reflect shared principles that validate our design strategy and suggest feasible trajectories for enhancement.

Once channel endothelialization is optimized, we plan to introduce KRIT-1 knockdown via siRNA transfection in BAECs. Comparing permeability in wild-type versus CCM-phenotyped channels under constant flow (10 dyne/cm²) will allow us to directly test the impact of genetic perturbation on endothelial barrier function. With sufficient validation, this system may serve as a platform for preclinical drug screening and pathophysiological analysis in CCM and related cerebrovascular disorders.

Conclusion

This study presents the development of a reproducible endothelialized 3D hydrogel channel designed to model the cerebral microvascular environment relevant to cerebral cavernous malformations. Through careful hydrogel formulation, mold design, and preliminary permeability and adhesion testing, we established the groundwork for a robust in vitro model. While challenges remain, such as improving imaging accuracy and achieving full endothelialization, the platform demonstrates strong potential for disease modeling and future genetic manipulation. With refinement, this system may enable more precise studies of CCM pathogenesis and therapeutic screening within a physiologically relevant, controlled microenvironment.

End Matter

Author Contributions and Notes

Z.A.L. and A.L.B. designed research with help from B.P.H., Z.A.L. and A.L.B performed research, A.L.B. and Z.A.L. analyzed data; and Z.A.L. and A.L.B. wrote the paper.

The authors declare no conflict of interest.

Acknowledgments

Brian P. Helmke, Phd
Christopher B. Highley, Phd

References

Andresen Eguiluz, R. C., Kaylan, K. B., Underhill, G. H., & Leckband, D. E. (2017). Substrate stiffness and VE-cadherin mechano-transduction coordinate to regulate endothelial monolayer integrity. Biomaterials, 140, 45–57. https://doi.org/10.1016/j.biomaterials.2017.06.010

Awad, I. A., & Polster, S. P. (2019). Cavernous angiomas: Deconstructing a neurosurgical disease. https://doi.org/10.3171/2019.3.JNS181724

Bellis, S. L. (2011). Advantages of RGD peptides for directing cell association with biomaterials. Biomaterials, 32(18), 4205–4210. https://doi.org/10.1016/j.biomaterials.2011.02.029

Caro, C. G., Fitz-Gerald, J. M., & Schroter, R. C. (1969). Arterial Wall Shear and Distribution of Early Atheroma in Man. Nature, 223(5211), 1159–1161. https://doi.org/10.1038/2231159a0

Caton, M. T., & Shenoy, V. S. (2024). Cerebral Cavernous Malformations. In StatPearls. StatPearls Publishing. http://www.ncbi.nlm.nih.gov/books/NBK538144/

Fallenstein, G. T., Hulce, V. D., & Melvin, J. W. (1969). Dynamic mechanical properties of human brain tissue. Journal of Biomechanics, 2(3), 217–226. https://doi.org/10.1016/0021-9290(69)90079-7

Fischer, A., Zalvide, J., Faurobert, E., Albiges-Rizo, C., & Tournier-Lasserve, E. (2013). Cerebral cavernous malformations: From CCM genes to endothelial cell homeostasis. Trends in Molecular Medicine, 19(5), 302–308. https://doi.org/10.1016/j.molmed.2013.02.004

Lee, J. H., Tachibana, T., Wadamori, H., Yamana, K., Kawasaki, R., Kawamura, S., Isozaki, H., Sakuragi, M., Akiba, I., & Yabuki, A. (2023). Drug-Loaded Biocompatible Chitosan Polymeric Films with Both Stretchability and Controlled Release for Drug Delivery. ACS Omega, 8(1), 1282–1290. https://doi.org/10.1021/acsomega.2c06719

Maderna, C., Pisati, F., Tripodo, C., Dejana, E., & Malinverno, M. (2022). A murine model of cerebral cavernous malformations with acute hemorrhage. iScience, 25(3), 103943. https://doi.org/10.1016/j.isci.2022.103943

National Institute of Neurological Disorders and Stroke. (2024, July 19). Cerebral Cavernous Malformations | National Institute of Neurological Disorders and Stroke. https://www.ninds.nih.gov/health-information/disorders/cerebral-cavernous-malformations

Qiu, Y., Ahn, B., Sakurai, Y., Hansen, C. E., Tran, R., Mimche, P. N., Mannino, R. G., Ciciliano, J. C., Lamb, T. J., Joiner, C. H., Ofori-Acquah, S. F., & Lam, W. A. (2018). Microvasculature-on-a-chip for the long-term study of endothelial barrier dysfunction and microvascular obstruction in disease. Nature Biomedical Engineering, 2, 453–463. https://doi.org/10.1038/s41551-018-0224-z

Sahoo, T., Johnson, E. W., Thomas, J. W., Kuehl, P. M., Jones, T. L., Dokken, C. G., Touchman, J. W., Gallione, C. J., Lee-Lin, S. Q., Kosofsky, B., Kurth, J. H., Louis, D. N., Mettler, G., Morrison, L., Gil-Nagel, A., Rich, S. S., Zabramski, J. M., Boguski, M. S., Green, E. D., & Marchuk, D. A. (1999). Mutations in the gene encoding KRIT1, a Krev-1/rap1a binding protein, cause cerebral cavernous malformations (CCM1). Human Molecular Genetics, 8(12), 2325–2333. https://doi.org/10.1093/hmg/8.12.2325

Skelton, M. L., Gentry, J. L., Astrab, L. R., Goedert, J. A., Earl, E. B., Pham, E. L., Bhat, T., & Caliari, S. R. (2024). Modular Multiwell Viscoelastic Hydrogel Platform for Two- and Three-Dimensional Cell Culture Applications. ACS Biomaterials Science & Engineering, 10(5), 3280–3292. https://doi.org/10.1021/acsbiomaterials.4c00312

Yi, B., Xu, Q., & Liu, W. (2022). An overview of substrate stiffness guided cellular response and its applications in tissue regeneration. Bioactive Materials, 15, 82–102. https://doi.org/10.1016/j.bioactmat.2021.12.005

Supplementary Materials

Figure 1. Graph comparing the storage modulus between a 2% and 3% NorHA hydrogel across oscillation strain

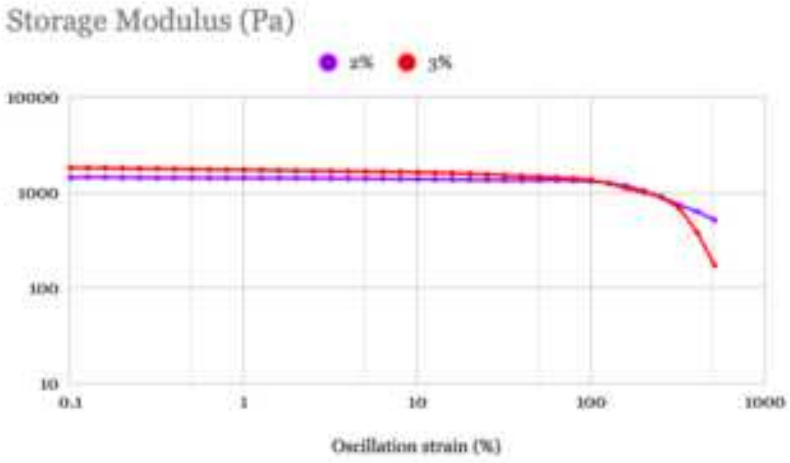

Figure 2. Graph comparing the loss modulus between a 2% and 3% NorHA hydrogel across oscillation strain

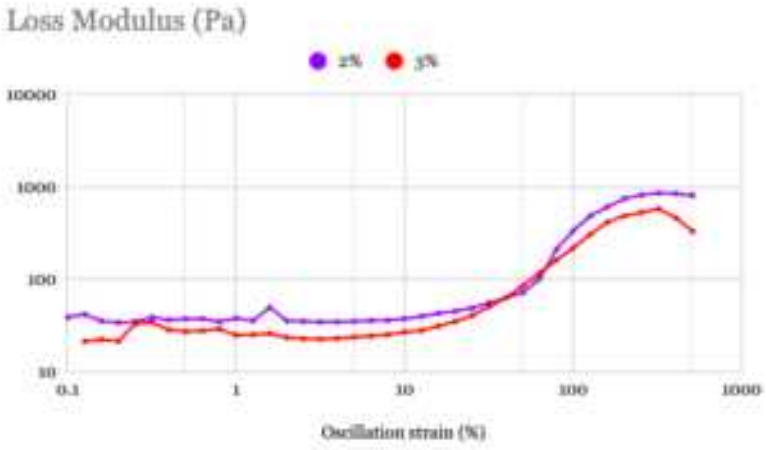

Figure 3. Resin printed mold of our CAD design with wells and its associated PDMS device

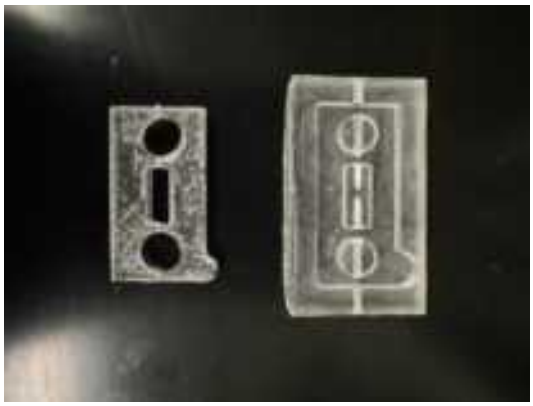

Figure 4. CAD design of the resin-printed mold intended for general hydrogel and FITC-dextran tests

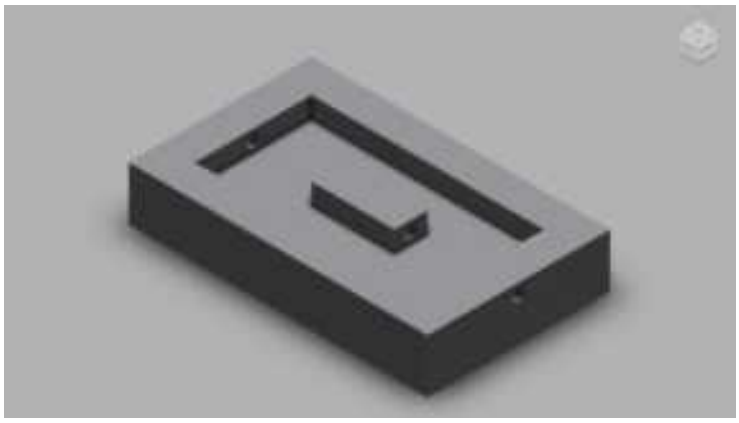

Figure 5. CAD design of the resin-printed mold with wells intended for cell experiments

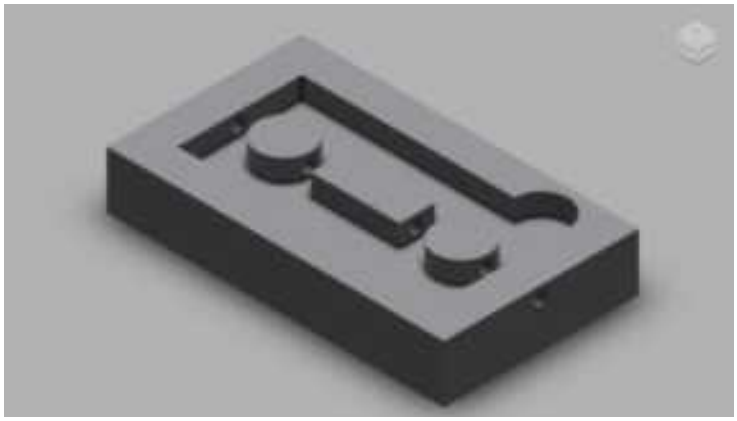

Figure 6. Resin-printed mold of our CAD design with its associated PDMS device, intended for 22-gauge needle insertion

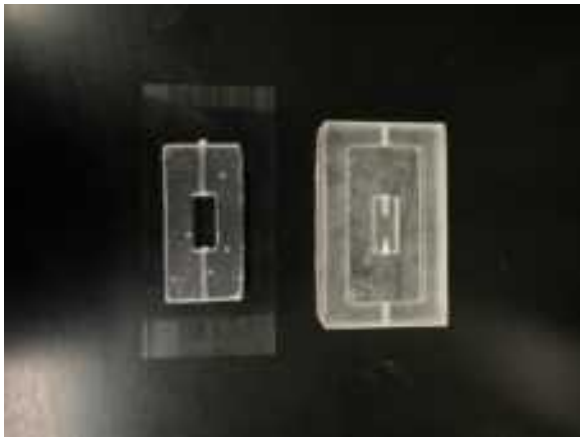

Figure 7. Schematic of hydrogel fabrication and channel development provided by Lauren Porter